Dios, M. de, González, Z., Gordo, E., Ferrari, B. (2015). Core-shell Ti(C,N)-Ni Structures Fabricated by Chemical Precipitation of Ni-based Nanoparticles on Ti(C,N) Suspensions. *Euro PM2015 Proceedings: Hard Materials, Alternative Binders*. EPMA, 2015

Euro PM2015 – Hard Materials – Alternative Binders

Manuscript refereed by Dr Ralph Useldinger (Ceratizit SA, Luxembourg)

Core-shell Ti(C,N)-Ni Structures Fabricated by Chemical Precipitation of Ni-based Nanoparticles on Ti(C,N) Suspensions

M.Dios[a,], Z.González[b], E.Gordo[a], B.Ferrari[b]*
a Materials Science and Engineering and Chemical Engineering Department, University Carlos III, Avda. Universidad 30, 28911 Leganés, Madrid, Spain
b Ceramic and Glass Institute, CSIC, C/Kelsen 5, 28049 Madrid, Spain

Abstract
Ti(C,N)-based cermets are currently used in high-speed cutting tools industry due to their high thermal stability. In previous works, Fe was proposed as metal matrix, however the use of iron as continuous matrix strongly affects the processing due to the low wetting capability of molten Fe with the reinforcement phase, Ti(C,N). To solve this problem the use of alloys such as FeNi has been proposed, where Ni improves the wettability between the ceramic and the metal phases. This work proposes a bottom-up approach to build the cermet microstructure through the synthesis of metal nanoparticles on the surface of Ti(C,N) micrometric particles, creating core-shell Ti(C,N)-Ni structures. For that purpose, synthesis parameters to obtain Ni nanoparticles were optimized and then, a one-pot synthesis procedure was tested to obtain core-shell Ti(C,N)-Ni particles by the chemical precipitation of Ni nanoparticles onto the surface of micronic Ti(C,N) particles previously stabilized in an aqueous suspension. Nickel nanoparticles and subsequent core-shell were characterized by measuring the particle size by Dynamic Light Scattering (DLS), X-Ray Diffraction (XRD), field emission scanning electron microscopy (FE-SEM).

1. Introduction

Compared to cemented carbides, Ti(C,N)-based cermets are gaining increasing technical importance [1, 2], due to their excellent combination of hardness at high temperature, strength, wear resistance and thermal conductivity [3]. However, titanium carbonitride-based cermets present some disadvantages such as low toughness, and low sintering behavior. Fe-based cermets present low sintering performance due to poor wettability of the liquid phase and the risk of producing reaction products with the reinforcement that lead to embrittlement [4]. Additions of some nanometric elements or compounds can improve the sintering performance by improving the wettability between the ceramic and the liquid phase, enhance density and decrease particle growth rate such as Ni, Mo or a great variety of binary carbides such as Mo_2C, WC, TaC or NbC [1, [3-6]].

Sintering of nanoparticles has aroused some significant attention in research and industry. The main challenge is to avoid coarsening during the sintering process so that the nanostructure can be maintained. There is a wide range of manufacturing methods to obtain nanoparticles (<100nm). Some of them are based on physical processes such as spray pyrolysis [7, 9], mechanical milling [10] and physical vapor deposition (PVD) [11, 12], whereas others are based on chemical processes. The later have been extensively used for synthesis of ultra-fine powders for industrial applications because they are very versatile to apply for several kinds of materials with higher productivity and with relatively low cost. These chemical synthesis methods include electrochemical processes [12], chemical vapor deposition (CVD) [[12]–[14]], mechano-chemical [15] and electroless processes [[16]–[18]]. However, most of these methods are not convenient for the massive production of fine metal powders due to the technical difficulties and the expensive equipment involved.

The electroless nickel plating method is now widely used to modify the surface of various materials such as nonconductors, semiconductors and metals. The cost of this plating method is low, and the process yields a uniform coating over all surfaces of any profile of metallic or electrically non-conductive materials. This technique has also attracted substantial interest in both micro and nano fabrication, in optics and in the decoration on carbon nanotubes, SiC and other kinds of powders [19]. Metal-coated ceramic powders refer to composite powders with a ceramic core and a metallic shell that can endow the ceramic powders with particular electrical, magnetic and chemical properties and can simultaneously improve the wetting properties between metal and ceramic materials. In this connection, electroless nickel plating has been recognized as one of the most effective techniques for preparing metal-coated ceramics powders [20-21]. Recently, core–shell structures have been fabricated successfully in a number of materials with various methods, including self-assembly, the sonochemical method, vapor deposition polymerization, the seed-mediated growth technique and the chemical vapor–liquid reaction.

According to the needs for the desired properties, core-shell structures have been designed by the chemical precipitation of Ni nanoparticles (NP's) onto the surface of micronic Ti(C,N) particles previously stabilized in an aqueous suspension. The electroless chemical reduction on Ni^{2+} salt was carried out for the preparation of fine

nickel NP's from the aqueous solution by reducing with hydrazine. Moreover, in order to optimize the coverage of Ti(C,N) surface by the Ni NP's, the influence of the synthesis variables (ion nickel concentration, reducing agent ratio, temperature and time of the synthesis and ultrasound effect) were evaluated.

In this work, unlike to what has been commonly found in literature [8], [14], [22]–[30], the electroless chemical reduction was modified in two main aspects. On the one hand, the synthesis were carried out in aqueous solution, avoiding the use of any other kind of solvent as ethanol, methanol, resulting an environmentally friendly route, and on the other hand, nickel nitrate was used as Ni precursor instead of the more common use of chlorides and acetates, harmful precursors to the metal matrix.

2. Experimental procedure

2.1 Materials

The raw materials used were Nickel nitrate hexahydrate ($Ni(NO_3)_2 \cdot 6H_2O$) and potassium hydroxide were received from Panreac Company, hydrazine monohydrate ($N_2H_4 \cdot H_2O$) was purchased from Sigma-Aldrich and titanium carbonitride (Ti(C,N) powder Grade C) was received from H.C. Starck GmbH. The water used in this work was deionized water. All chemicals used in these experiments were of reagent grade and used without any further purification.

2.2 Synthesis of nickel nanoparticles

A typical preparation procedure is described as follow: a desired amount of nickel nitrate hexahydrate was dissolved into deionized water (**solution a**). Another mixture was obtained by mixing potassium hydroxide previously dissolved in water and hydrazine monohydrate together (**mixture b**). Then, mixture b, was poured into solution a immediately with continued and vigorous ultrasonic power at controlled temperature, through the recirculation of a continuous flow of water from a cryothermal bath, all in a total solution volume of 50 mL. The overall reaction times were 5 minutes or 60 minutes depending on the synthesis. The resultant product was washed thoroughly with deionized water for removal of reaction residues followed by spin dry stages. The variables involved in the synthesis are:

- The concentration of nickel nitrate hexahydrate: **$[Ni^{2+}]$** = 0.02M, 0.05M, 0.075M and 0.1M
- The reductant agent (hydrazine monohydrate) - nickel nitrate hexahydrate ratio. **$[N_2H_4/Ni^{2+}]$**= 6, 20, 60.
- Temperature: **T**= 40 ºC - 50 ºC
- US Time: **t=** 5 min - 60 min
- US Power: **W=** 100% - 50%

2.3 Synthesis of Core-Shell Ti(C,N)-Ni

In this case, core-shell structures have been obtained by the chemical precipitation of Ni nanoparticles (NP's) onto the surface of micronic Ti(C,N) particles previously stabilized in the aqueous **solution a**.

2.4 Characterization of Ni nanoparticles and core-shell structures

A Zetasizer Nano ZS (Malvern, UK) was used in order to determine the particle size distribution and zeta potential of Ni nanoparticles using Dynamic Light Scattering (DLS) and laser Doppler velocimetry, respectively. Suspensions used for determination were prepared with concentrations of 0.1 g/L using 10^{-2} M KCl as solvent and inert electrolyte, so as to maintain the ionic strength of the medium. The pH adjustments of the suspensions were carried out by addition of small quantities of 0.1M HNO_3 or TMAH (Tetramethylammonium Hydroxide) and controlled with a pH probe (Metrohm AG, Germany). Subsequently, homogenization was achieved by sonication, using a UP400S Ultrasonic probe (Hielscher, Germany) for an optimized period of time.

Particle size and morphology were also examined by field emission scanning electron microscopy (FE-SEM) in an S-4700 microscope (Hitachi, JAPAN) and by high-resolution transmission electron microscopy (HRTEM) in a JEOL JEM 2011 (Jeol Ltd., Japan).

Finally, crystalline phase was characterized by X-ray diffraction (Siemens-Bruker D8 Advance, Germany) using Cu K_α radiation (λ=1.540598 Å). The diffraction patterns were measured step by step (0.05º in 2Θ).

3. Results and discussion

3.1 Synthesis of Ni nanoparticles

The X-Ray Diffraction pattern of metallic nickel is shown in Figure 1. This pattern is representative of all the

samples obtained from different experiments, showing the three characteristic peaks of FCC nickel (45º, 52.4º, 76.9º), corresponding to Miller indices (111), (200) and (222) respectively according to the index card JCPDS nº 04-0850. This indicates that all the products obtained are pure face-centered cubic (FCC) metallic nickel without any other impurity. Besides, in contrast to what it is commonly found in the literature, the yield has remained constant in all the syntheses that have been carried out, settling at around 80-85%.

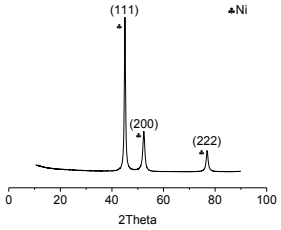

Figure 1 X-Ray Diffraction pattern of nickel

Although nickel has been obtained in all syntheses carried out, the study of the different synthesis parameters have shown some differences that should be highlighted, as can be seen in Table 1.

Study	Molar ratio (Ni^{2+}/KOH/N_2H_4)	Time (min)	T (ºC)	[Ni^{2+}] (M)	P [W] (%)	Yield (%)	Dmeb (nm)	Dn50 (nm)	Dv50 (nm)	
[Ni^{2+}]	1/10/60	60	40	**0.1**	100	77.8	300	105	122	615
	1/10/60	60	40	**0.075**	100	84.4	200	90	91	531
	1/10/60	60	40	**0.05**	100	74.9	150	80	79	458
	1/10/60	60	40	**0.02**	100	-	-	-	-	-
[N_2H_4]	**1/10/60**	60	40	0.05	100	74.9	150	80	79	458
	1/10/20	60	40	0.05	100	76	100	115	164	712
	1/10/6	60	40	0.05	100	-	-	-	-	-
US Time	1/10/60	**60**	50	0.1	100	83.5	400	300	342	615
	1/10/60	**5**	50	0.1	100	84.3	300	90	105	458
Temperature	1/10/60	60	**40**	0.1	100	77.8	300	100	105	615
	1/10/60	60	**50**	0.1	100	83.5	400	300	342	615
W	1/10/60	5	50	0.1	**100**	84.3	300	90	105	458
	1/10/60	5	50	0.1	**50**	78.2	200	140	164	615

Table 1 Synthesis conditions of Ni nanoparticles and results

Effect of the initial [Ni^{2+}]

A reaction scheme in the present research is expected to include the formation of $Ni(OH)_2$ from $Ni(NO_3)_2{\cdot}6H_2O$, the dissolution of $Ni(OH)_2$, the reduction of dissolved nickel species and then the nucleation and growth of the nickel particles from the aqueous solution. The chemical reaction can be formulated as follows in Equation 1.

$$2Ni^{2+} + 4OH^- + N_2H_4 \rightarrow 2Ni + N_2 + 4H_2O$$ **Equation 1 Chemical reaction**

It was found that the **induction time**, when starting turning the solution's color to black, i.e. when it has started to precipitate metallic nickel nanoparticles, shortened with the increasing the molar concentration of $Ni(NO_3)_2{\cdot}6H_2O$ supporting the theory that the lower amount of ion nickel, the slower reaction kinetics. It was also determined a threshold for the ion nickel concentration; If ion nickel concentration is lower than 0.05M, the concentration will be so low that there will not be enough atoms to form stable nuclei, so no nickel particles could form, and the synthesis does not occur in a reasonable time.

In contrast to what is reported in some papers [[14], [18]], the lower the ion nickel concentration, the smaller nanoparticles, as it can be seen in Figure 2. The results showed fit well with the studies made by Da-Peng Wang [25] for the nickel sulfate ($NiSO_4$). The reason may be that at the beginning, the reaction kinetic was slow, and only limited nuclei were formed; and the increasing nickel concentration speeds up it is Ostwald Ripening growth from 80nm to 90-105nm. Besides the solvation and the particle's surface potential cannot inhibit agglomeration [29]. Therefore, the primary particles reduced from the solution are not stable and will grow by coagulation forming hard agglomerates of plates, as it is shown Figure 2 (c). This effect will increase if higher ion nickel concentrations are used.

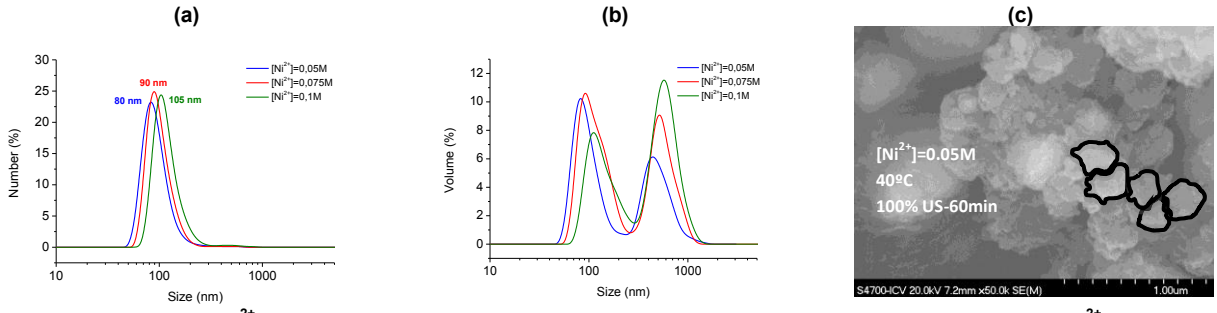

Figure 2 Effect of initial [Ni^{2+}] on Dn50 (a) and Dv50 (b) and FESEM micrograph of the sample obtained with [Ni^{2+}]=0.05M (c)

Effect of the [N_2H_4/Ni^{2+}] ratio

Supporting the theory that the hydrazine is the agent responsible of the reduction reaction, the induction time, when starting turning the solution's color to black, shortened with the increasing the molar concentration of N_2H_4. This result was also obtained by Li et al. in the synthesis of nickel chloride ($NiCl_2$) [23].
When reducing the hydrazine concentration, the formation of larger particles could be attributed to the fact that the reduction rate of the nickel nitrate was slow and only few nuclei were formed in the early period of the reduction. The atoms formed at that period might participate mainly in collisions with already formed nuclei, instead of the formation of new nuclei. However, by increasing hydrazine concentration, the reduction rate increases due to the generation of much more nuclei and the formation of smaller (from 115nm to 80nm) and less agglomerated nickel nanoparticles, as it can be seen in Figure 3.
When the concentration ratio of hydrazine to nickel nitrate was large enough, the reduction rate of nickel nitrate was much faster than the nucleation rate and almost all nickel ions were reduced to atoms before the formation of nuclei.

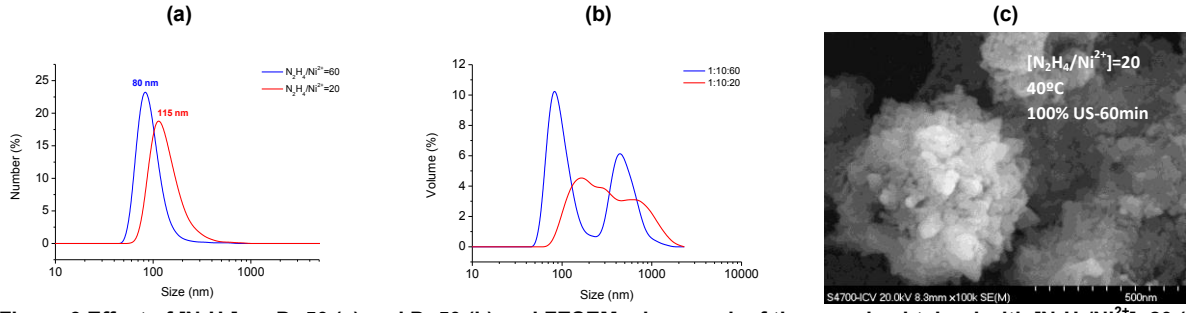

Figure 3 Effect of [N_2H_4] on Dn50 (a) and Dv50 (b) and FESEM micrograph of the sample obtained with [N_2H_4/Ni^{2+}]=20 (c)

Effect of the temperature

Regardless of the synthesis temperature, both syntheses turned the solution's color to black during application of the ultrasound stage. However, higher synthesis temperatures, will be employed by the nanoparticles in increase their size and agglomerate the existent particles, as it is shown in Figure 4.
This tendency may be related to the increase of dissolution rate and reduction rate in the solution and the decrease of solubility with the increasing reaction temperature. Larger particles may be formed though two processes: the growth of primary particles and the coalescence of primary particles. As a consequence of the reaction temperature rise, the dissolution rate of the intermediate compound, the reduction rate in the solution, and then the nucleation rate increase. Therefore, the number of primary particles formed during the nucleation stage increases. Finally, the larger particles may be formed by the coalescence of primary particles rather than the growth of primary particles due to the decrease of solubility in the solution with increasing reaction temperature.

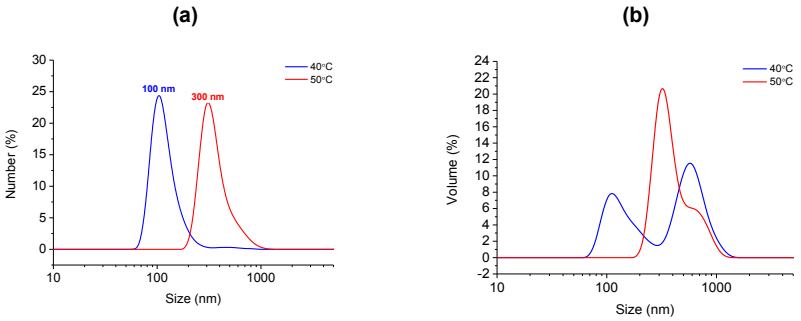

Figure 4 Effect of the temperature on Dn50 (a) and Dv50(b)

Effect of the ultrasonic power and time

Both time and ultrasonic power have a great influence on the particle size and agglomeration state of the nanoparticles. On one hand, the higher the ultrasonic power applied to the synthesis, the greater will be the dispersion of the nanoparticles due to the more energetic shock waves produced by the probe, reducing the size and the agglomeration state of the nanoparticles. However, invariably some agglomeration occurs at the nucleation stage; nuclei possess a high surface area to volume ratio, and due to this some nuclei tend to reduce it by adhering to another one. On the other hand, the complete reduction of the nanoparticles will occur before the first five minutes of synthesis, because of this, the rest of the time, will be employed by the nanoparticles in increase their size and agglomerate the existent particles, as it is shown in Figure 5.

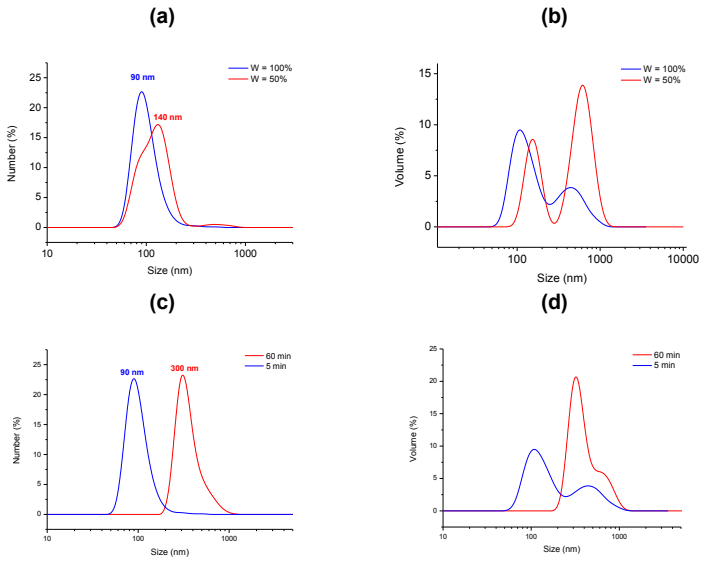

Figure 5 Effect of the ultrasonic power and time respectively on Dn50 (a and c) and Dv50 (b and d)

3.2 Synthesis of core-shell Ti(C,N)-Ni

Aiming to create core-shell particles, the optimal route to obtain the most suitable nickel NP's was used. As it can be seen in Figure 6 core-shell structures have been obtained by the chemical precipitation of Ni nanoparticles (NP's) onto the surface of micronic Ti(C,N) particles previously stabilized.

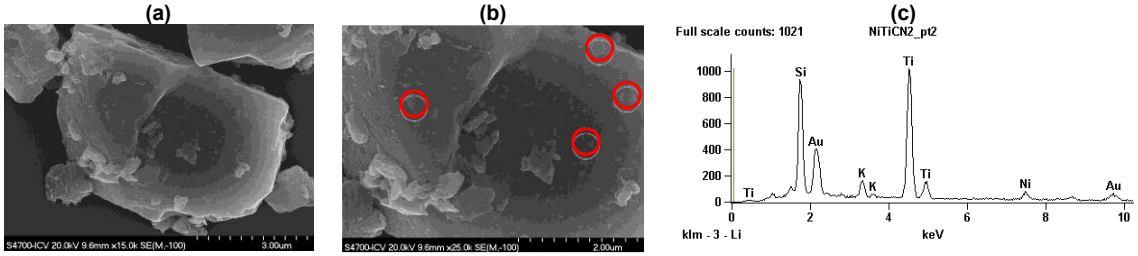

Figure 6 FESEM micrograph of the core-shell Ti(C,N)-Ni (a) y (b) and EDX analysis of the sample (c)

4. Conclusions

- The synthesis of Ni NP's by a reduction method using hydrazine as reductor agent in aqueous medium has been successfully achieved. Although the amount of hydrazine for the synthesis of Ni NP's is considerably higher than other previously reported (R=60), the synthesis of pure Ni NP's, 80 nm in diameter, was carried out in shorter times (up to 5min).
- Ti(C,N)-Ni Core-Shells were obtained providing a route for the bottom up design of FeNi-Ti(C,N) interphases in cermets.

Acknowledgements
The authors acknowledge the support of the projects S2013/MIT-2862 and MAT2012-38650-C02-01, MAT2012-38650-C02-02. M. de Dios acknowledges MINECO through the grant FPI-2013 and Dr. Z González acknowledges to MINECO through the grant PTQ-13-05985.

References
[1] P. Ettmayer, H. Kolaska, W. Lengauer, and K. Dreyer, "Ti(C,N) cermets — Metallurgy and properties," *Int. J. Refract. Met. Hard Mater.*, vol. 13, pp. 343–351, 1995.
[2] A. Bellosi, R. Calzavarini, M. G. Faga, F. Monteverde, C. Zancolò, and G. E. D'Errico, "Characterisation and application of titanium carbonitride-based cutting tools," *J. Mater. Process. Technol.*, vol. 143–144, pp. 527–532, 2003.
[3] S. Zhang, "Titanium carbonitride-based cermets: processes and properties," *Mater. Sci. Eng. A*, vol. 163, pp. 141–148, 1993.
[4] J. Antonio and E. Quintana, "Diseño de microestructuras complejas metal-cerámica en base hierro por procesamiento coloidal en agua,"
[5] I. a. Ibrahim, F. a. Mohamed, and E. J. Lavernia, "Particulate reinforced metal matrix composites - a review," *J. Mater. Sci.*, vol. 26, pp. 1137–1156, 1991.
[6] P. Alvaredo, D. Mari, and E. Gordo, "High temperature transformations in a steel-TiCN cermet," *Int. J. Refract. Met. Hard Mater.*, vol. 41, pp. 115–120, 2013.
[7] V. . Tracey, "Nickel in hardmetals," *Int. J. Refract. Met. Hard Mater.*, vol. 11, no. August 1992, pp. 137–149, 1992.
[8] L. Bai, F. Yuan, and Q. Tang, "Synthesis of nickel nanoparticles with uniform size via a modified hydrazine reduction route," *Mater. Lett.*, vol. 62, pp. 2267–2270, 2008.
[9] X. Weng, D. Brett, V. Yufit, P. Shearing, N. Brandon, M. Reece, H. Yan, C. Tighe, and J. a. Darr, "Highly conductive low nickel content nano-composite dense cermets from nano-powders made via a continuous hydrothermal synthesis route," *Solid State Ionics*, vol. 181
[10] J. M. Córdoba, M. D. Alcalá, M. a. Avilés, M. J. Sayagués, and F. J. Gotor, "New production of TiCxN1-x-based cermets by one step mechanically induced self-sustaining reaction: Powder synthesis and pressureless sintering," *J. Eur. Ceram. Soc.*, vol. 28, pp. 2085–2098.
[11] C. Burda, X. Chen, and R. Narayanan, *Chemistry and Properties of Nanocrystals of Different Shapes - Chemic ... Chemistry and Properties of Nanocrystals of Different Shapes - Chemic ... Chemistry and Properties of Nanocrystals of Different Shapes*. 2005.
[12] S. F. Moustafa and W. M. Daoush, "Synthesis of nano-sized Fe-Ni powder by chemical process for magnetic applications," *J. Mater. Process. Technol.*, vol. 181, pp. 59–63, 2007.
[13] J. Gurland, "New scientific approaches to development of tool materials," *Int. Mater. Rev.*, vol. 33, no. 3, pp. 151–166, 1988.
[14] Z. G. Wu, M. Munoz, and O. Montero, "The synthesis of nickel nanoparticles by hydrazine reduction," *Adv. Powder Technol.*, vol. 21, no. 2, pp. 165–168, 2010.
[15] K. Byrappa and T. Adschiri, "Hydrothermal technology for nanotechnology," *Prog. Cryst. Growth Charact. Mater.*, vol. 53, pp. 117–166.
[16] J. Sudagar, J. Lian, and W. Sha, "Electroless nickel, alloy, composite and nano coatings - A critical review," *J. Alloys Compd.*, vol. 571, pp. 183–204, 2013.
[17] T. Cetinkaya, M. Uysal, M. O. Guler, H. Akbulut, and A. Alp, "Improvement cycleability of core-shell silicon/copper composite electrodes for Li-ion batteries by using electroless deposition of copper on silicon powders," *Powder Technol.*, vol. 253, pp. 63–69, 2014.
[18] R. C. Agarwala and V. Agarwala, "Electroless alloy / composite coatings : A review," *Sadhana*, vol. 28, no. August, pp. 475–493.
[19] M. Uysal, R. Karsliolu, a. Alp, and H. Akbulut, "Nanostructured core-shell Ni deposition on SiC particles by alkaline electroless coating," *Appl. Surf. Sci.*, vol. 257, pp. 10601–10606, 2011.
[20] G. P. Ling and Y. Li, "Influencing factors on the uniformity of copper coated nano-Al 2O3 powders prepared by electroless plating," *Mater. Lett.*, vol. 59, pp. 1610–1613, 2005.
[21] Y. Q. Kang, M. S. Cao, J. Yuan, L. Zhang, B. Wen, and X. Y. Fang, "Preparation and microwave absorption properties of basalt fiber/nickel core-shell heterostructures," *J. Alloys Compd.*, vol. 495, no. 1, pp. 254–259, 2010.
[22] S. H. Wu and D. H. Chen, "Synthesis and characterization of nickel nanoparticles by hydrazine reduction in ethylene glycol," *J. Colloid Interface Sci.*, vol. 259, pp. 282–286, 2003.
[23] Z. Li, C. Han, and J. Shen, "Reduction of Ni2+ by hydrazine in solution for the preparation of nickel nano-particles," *J. Mater. Sci.*, vol. 41, pp. 3473–3480, 2006.
[24] J. W. Park, E. H. Chae, S. H. Kim, J. H. Lee, J. W. Kim, S. M. Yoon, and J. Y. Choi, "Preparation of fine Ni powders from nickel hydrazine complex," *Mater. Chem. Phys.*, vol. 97, pp. 371–378, 2006.
[25] D. P. Wang, D. B. Sun, H. Y. Yu, and H. M. Meng, "Morphology controllable synthesis of nickel nanopowders by chemical reduction process," *J. Cryst. Growth*, vol. 310, pp. 1195–1201, 2008.
[26] R. Y. Chen and K. G. Zhou, "Preparation of ultrafine nickel powder by wet chemical process," *Trans. Nonferrous Met. Soc. China (English Ed.*, vol. 16, no. 50474047, pp. 1223–1227, 2006.
[27] Z. Libor and Q. Zhang, "The synthesis of nickel nanoparticles with controlled morphology and SiO 2/Ni core-shell structures," *Mater. Chem. Phys.*, vol. 114, no. 2, pp. 902–907, 2009.
[28] H. Kim Kwang Ho, Y. B. Lee, S. G. Lee, H. C. Park, and S. S. Park, "Preparation of fine nickel powders in aqueous solution under wet chemical process," *Mater. Sci. Eng. A*, vol. 381, pp. 337–342, 2004.
[29] K. H. Kim, Y. B. Lee, E. Y. Choi, H. C. Park, and S. S. Park, "Synthesis of nickel powders from various aqueous media through chemical reduction method," *Mater. Chem. Phys.*, vol. 86, pp. 420–424, 2004.
[30] W. Xu, K. Y. Liew, H. Liu, T. Huang, C. Sun, and Y. Zhao, "Microwave-assisted synthesis of nickel nanoparticles," *Mater. Lett.*, vol. 62, pp. 2571–2573, 2008.